Full title:

Evaluation of the second-generation whole-heart motion correction algorithm (SSF2) used to demonstrate the aortic annulus on cardiac CT

Short title:

Clinical utility of SSF2 in the aortic annulus

Authors:

Yoriaki Matsumoto[1*)], Chikako Fujioka[1)], Kazushi Yokomachi[1)], Nobuo Kitera[1)], Eiji Nishimaru[1)], Masao Kiguchi[1)], Toru Higaki[2)], Ikuo Kawashita[2)], Fuminari Tatsugami[2)], Yuko Nakamura[2)], Kazuo Awai[2)]

1) Department of Radiology, Hiroshima University Hospital, Kasumi, Minami-ku, Hiroshima, Japan.

2) Department of Diagnostic Radiology, Graduate School of Biomedical and Health Sciences, Hiroshima University, Kasumi, Minami-ku, Hiroshima, Japan.

18 * Corresponding author

19 E-mail: yoriaki@hiroshima-u.ac.jp (YM)

20

Abstract

Purpose: To investigate the usefulness of the second-generation whole-heart motion correction algorithm (SnapShot Freeze 2.0, SSF2) for demonstrating the aortic annulus at pre-transcatheter aortic valve implantation cardiac CT.

Method: We retrospectively analyzed 90 patients with severe aortic stenosis who had undergone cardiac CT on a 256-row CT scanner. The patients were divided into the 3 groups based on their heart rate during the scan (low, < 60 bpm, n = 30; intermediate, 60-69 bpm, n = 30; high, >70 bpm, n = 30). Image datasets were obtained at 40% and 75% of the R-R interval using standard and SSF2 reconstruction. The edge rise distance (ERD) on the CT attenuation profile of the aortic annulus was compared on images subjected to standard- and SSF2 reconstructions. The standard deviations (SD) of area and perimeter were compared using the *F*-test. The image quality was assessed by two observers using a 5-point Likert score.

Results: In patients with intermediate and high heart rates, the ERD was significantly shorter on SSF2- than standard reconstructed images ($p < 0.01$). The SD of area and perimeter were significantly smaller in SSF2 reconstruction than in standard (all: $p < 0.05$). Except for R-R interval 75% in patients with low heart rate ($p = 0.54$), the image quality scores were significantly higher for images reconstructed with SSF2 than

standard ($p < 0.01$).

Conclusions: For the demonstration of the aortic annulus in patients with high heart rate or a 40% R-R interval, SSF2- was superior to standard reconstruction.

Abbreviations: bpm: beats per minute, CT: computed tomography, CNR: contrast-to-noise ratio, ERD: edge rise distance, MPR: multiplanar reconstruction, ROI: region of interest, SD: standard deviation, SSF: SnapShot Freeze, TAVI: transcatheter aortic valve implantation

Introduction

Electrocardiogram-gated cardiac computed tomography (CT) scans are important for planning the transcatheter aortic valve implantation (TAVI) procedure in patients with severe aortic stenosis [1, 2]. However, motion artifacts present a technical challenge because they can compromise the assessment of structures such as the coronary arteries and valves, especially in patients with a high heart rate [3-7]. Inaccurate sizing increases the risk of complications such as perivalvular leak or rupture in TAVI patients [2, 8, 9]. Precise pre-procedural imaging is therefore crucial to assure optimal patient outcome [2, 9]. To avoid motion artifacts, the society of cardiovascular CT guidelines [10] recommend that the heart rate be controlled to be less than 60 beats per minute (bpm) by the oral or intravenous administration of a β-blocker. To correct motion artifacts, technical advances in CT systems have improved the temporal resolution, increased the gantry rotation speed, and applied dual-source CT and multi-segment reconstruction; software solutions have been developed [11].

The first-generation motion correction algorithm (SnapShot Freeze, SSF1; GE Healthcare) is vendor-specific and designed to address coronary motion artifacts on cardiac scans. Its application significantly improved the image quality of the coronary arteries in patients with a high heart rate [12-19]. A second-generation vendor-specific

66 motion correction algorithm (SnapShot Freeze 2.0, SSF2; GE Healthcare) extended the
67 motion correction range to the whole heart within one scan volume [20, 21]. We
68 examined whether the SSF2 algorithm improves the image quality of cardiac CT scans
69 acquired to evaluate not only the coronary arteries but also the aortic valves. We
70 enrolled patients with severe aortic stenosis who had undergone pre-TAVI standard
71 cardiac CT studies without motion correction and pre-TAVI scans subjected to SSF2
72 reconstruction and compared their image quality.
73

Materials and methods

This retrospective study (No. E-2623, Clinical study of motion correction algorithm for cardiac CT) was approved by our institutional review board; informed patient consent for the analyses was waived.

Study population

We enrolled 108 patients with severe aortic stenosis who underwent cardiac CT as candidates for TAVI between April 2021 and February 2022. Inclusion criteria were patients who underwent contrast-enhanced cardiac CT. Our exclusion criteria were severe renal failure (estimated glomerular filtration rate < 30 ml/min/1.73 m^2, 15 patients), poor breath holding during scanning (1 patient), extravasation during contrast injection (1 patient) or refusal of CT examination (1 patient). Thus, the final study population consisted of 90 patients; they were 33 male and 57 female ranging in age from 70 to 95 years (median age, 84 years).

To perform stratified analysis of the effect of SSF2 on heart rate during scanning, we divided 90 patients into 3 groups to include the same number of patients according to the relationship between heart rate and image quality [10, 12, 17, 18, 20, 22-24]. In group 1 (n = 30) the heart rate was low (< 60 bpm, range 34 -59 bpm), in group 2 (n =

30) it was intermediate (60 - 69 bpm), and in group 3 (n = 30) it was high (70 bpm or higher, range 70 - 119 bpm).

CT scanning

All patients were scanned on a 256-detector row CT scanner (Revolution CT; GE Healthcare, Milwaukee, WI, USA); prospective electrocardiogram-gated axial scans were acquired. The scanning- and reconstruction parameters were tube voltage, 120 kVp; tube current, selected by automatic tube current modulation (Smart-mA, GE Healthcare) based on the scout image; noise index, 25; detector collimation, 256 × 0.625 mm or 224 × 0.625 mm depending on the patient's heart size; gantry rotation, 0.28 seconds; slice thickness, 0.625 mm; scan field of view, 360 mm; display field of view, 200 mm; matrix, 512 × 512; reconstruction, half; reconstruction kernel, HD standard; reconstruction method, deep learning image reconstruction (TrueFidelity, strength High; GE Healthcare) [25-28]. The padding range was 0 - 100% of the R-R interval when a heart rate of less than 60 bpm was recorded during pre-examination monitoring; when it exceeded 60 bpm or was variable. In the presence of arrhythmia the padding range was 0 - 250%. All scans were craniocaudal from the tracheal bifurcation to the level of the inferior margin of the cardiac apex. All patients were able to perform

breath-holds during the examination. To achieve high image quality with minimal radiation doses, patients with a heart rate above 60 bpm 5 minutes before the start of scanning were given 2 - 10 mg propranolol hydrochloride (Inderal; Taiyo Holdings Co., Ltd., Tokyo, Japan).

The contrast medium (iodine concentration 350 mg/ml; Iomeron-350; Eisai Co., Ltd., Tokyo, Japan) was injected in triple-phase through a 20- or 22-gauge catheter into the antecubital vein using a power injector (Dual Shot type GX; Nemoto Kyorindo, Tokyo, Japan). The iodine dose of 273 mg/kg in the first phase was administered in 13 seconds. This injection was followed at a speed of 5 seconds by a 50/50 mix of contrast medium (53 mgI/kg) and saline, and finally 100% saline was delivered at the same injection speed. The scanning delay was determined with a bolus-tracking method. A round, approximately 400 mm^2 region of interest (ROI) was placed in the center of the left atrium and left ventricle, respectively. Scanning was started manually 1 second after contrast enhancement exceeded a predefined threshold of 300 Hounsfield units.

Data processing

Similar to the SSF1 algorithm [17, 19], the SSF2 algorithm uses data from adjacent cardiac phases (64 milliseconds before and after the target phase) to

128 characterize and correct the motion. The SSF2 algorithm, a fully automated technique
129 based on information and feedback obtained from SSF1 scans, seeks each region at all
130 image volumes for a local path that is consistent with the subset of measured data. Once
131 the vessel's motion path is identified, the data are discretized into a series of datasets
132 based on when the corresponding projection rays were measured. Each volume dataset
133 in the series undergoes spatial deformation by the motion field. This allows the motion
134 state to be mapped from the respective time to the central reference time, which is
135 determined by the prescribed cardiac phase [29].

136 All images were reconstructed using the standard (without motion correction)
137 algorithm with deep-learning image reconstruction for reducing the image noise [25-28].
138 For the cardiac phase, the systolic- (R-R interval, 40%) and diastolic phase (R-R
139 interval, 75%) used for pre-TAVI cardiac CT measurements were selected [2, 4, 29, 30].
140 As the systolic- and diastolic phases were additionally subjected to SSF2 reconstruction,
141 4 datasets were obtained for each patient. They were anonymized and transferred to the
142 workstation (Advantage Workstation 4.7, GE Healthcare) for later analysis.

143

144 ## Quantitative evaluation

145 The attenuation effect elicited by motion artifacts was analyzed at the aortic

146 annulus. All images were inspected by one radiological technologist (Y.M. with 15
147 years of experience with cardiac CT studies). To assess the aortic annulus, only axial-
148 and 2D double-oblique multiplanar reconstruction (MPR) images were examined. The
149 aortic annulus was defined as a virtual ring formed by joining the basal attachments of
150 the aortic leaflets [2, 31].

151 ## Edge rise distance

152 We generated a 3-directional CT attenuation profile (anterior-, superior-, and
153 inferior direction) of the aortic annulus (Fig 1) using the particle analysis tool (Plot
154 Profile) on the workstation (Ziostation2, Ziosoft, Tokyo, Japan). Areas of calcification
155 where CT attenuation fluctuates significantly were carefully avoided. The CT
156 attenuation profiles were generated at precisely the same location for images
157 reconstructed with standard and SSF2. We cut off the bottom and top 10% of the profile
158 and measured the 10 - 90% edge rise distance (ERD) [32, 33]. The ERD was examined
159 in three directions of the aortic annulus and the mean values were compared on
160 standard- and SFF2 images.

161

162 **Fig 1. Sample image of ERD.** Profile curve of the aortic annulus. The ERD at a pixel
163 attenuation from 10% to 90% of the maximum CT attenuation is shown. CT =

computed tomography; HU = Hounsfield units; ERD = edge rise distance

Dispersion of sizing

With respect to the sizing of the aortic annulus, we evaluated the dispersion between the two reconstructions. All images were analyzed by two radiological technologists (Y.M. and C.F., with 15 and 18 years of experience in cardiac CT imaging, respectively). They were blinded to presence of SSF2 technique and manually measured the aortic annulus area and perimeter of all patients independently on a CT workstation (Ziostation2, Ziosoft, Tokyo, Japan).

Contrast-to-noise ratio

To investigate the potential effect of SSF2 reconstruction on the quantitative ERD measurements, we inspected axial images and recorded the CT number and image noise [standard deviation (SD) of the CT number] in a circular ROI placed in the ascending aorta and septal wall of the ventricle. The size of the circular ROI cursor was as large as allowed by the diameter of the ascending aorta (approximately 5.0 - 10.0 mm^2) and of the septal wall of the ventricle (approximately 1.5 - 3.0 mm^2). Based on the obtained values we also calculated the contrast-to-noise ratio (CNR) using the formula: (CT number of the ascending aorta minus the CT number of the septal wall of the

ventricle) divided by the image noise of the ascending aorta [34].

Qualitative analysis

Two radiological technologists (Y.M. and C.F., with 15 and 18 years of experience in cardiac CT imaging, respectively) were blinded to presence of the SSF2 technique. They subjectively and independently inspected the MPR images from the sinotubular junction to the left ventricular outflow tract of the datasets for motion artifacts at the aortic annulus level. To grade the image quality they used the 5-point Likert scale where 1 = very poor (motion artifacts resulting in poor visualization of the aortic valve anatomy, not evaluable), 2 = poor (degraded visualization of the aortic valve anatomy due to motion artifacts, not evaluable), 3 = fair (minor motion artifacts with clear delineation of the aortic valve anatomy), 4 = good (no motion artifacts with confident identification of the aortic root anatomy including the cusp nadirs and annular contours), and 5 = excellent (outstanding image quality with a high level of diagnostic certainty with regard to the aortic valve cusps, the leaflet nadirs, and the detection of the aortic annular contours) [29]. Interobserver disagreement was resolved by consensus.

Statistical analysis

Continuous variables of demographic data, ERD, CT number, image noise and CNR are expressed as the median and range or as percentages or counts, aortic annulus area and perimeter or image quality scores as the mean and SD. The results of ERD, CT number, image noise, CNR and image quality scores were compared on images reconstructed with standard and SSF2 using the Mann-Whitney *U*-test. To compare the dispersion (SD) of area and perimeter between the two reconstructions we used the *F*-test. To determine whether the CNR was equivalent in standard and SSF2 reconstructions, we performed the equivalence test [35]. As the SD of the CNR between the proximal coronary arteries and the adjacent perivascular tissue was 5 in our earlier study [33], we adopted 5 as the equivalent margin. Interobserver agreement in the qualitative evaluation was classified as evaluable (score 3 - 5) and non-evaluable (score 1, 2) assessed with the Cohen kappa κ coefficient where a κ value of less than 0.20 = poor, 0.21 - 0.40 = fair, 0.41 - 0.60 = moderate, 0.61 - 0.80 = substantial, and 0.81 - 1.00 = near perfect agreement. All statistical analyses were performed with JMP 16 (SAS Institute Inc., Cary, NC, USA). Differences of $p < 0.05$ were considered statistically significant.

Results

Patient demographic data

As shown in Table 1, the median overall heart rate during CT image acquisition was 64 bpm (range: 34 - 119 bpm). Of the 90 patients, 70 were in sinus rhythm and 20 exhibited arrhythmias (atrial fibrillation, 19 patients; premature atrial contraction, 1 patient).

Table 1. Patient characteristics.

	Overall	Patients with low HR (<60 bpm)	Patients with intermediate HR (60-69 bpm)	Patients with high HR (>70 bpm)
Number of patients	90	30	30	30
Age (years)	84 (70-95)	85 (70-95)	84 (70-91)	84 (74-94)
Male, n (%)	33 (37%)	14 (42%)	11 (33%)	8 (25%)
Height (cm)	151 (130-169)	153 (137-167)	149 (130-169)	150 (135-169)
Body weight (kg)	51 (33-76)	50 (33-68)	53 (33-73)	52 (35-76)
Body mass index (kg/m^2)	22.4 (13.6-36.9)	21.7 (13.6-26.6)	22.9 (15.5-36.9)	22.7 (15.8-34.6)
estimated glomerular filtration rate (ml/min/1.73 m^2)	51.0 (30.3-115.5)	46.9 (30.3-115.5)	50.6 (31.3-87.3)	52.9 (31.0-82.8)
Heart rate during the scan (beats/min)	64 (34-119)	53 (34-59)	64 (60-69)	80 (70-119)
No. of patients with arrhythmias during the scan, n (%)	20 (22%)	6 (30%)	3 (15%)	11 (55%)

Atrial fibrillation, n (%)	19 (21%)	6 (31%)	3 (16%)	10 (53%)
Premature atrial contraction, n (%)	1 (1%)	0 (0%)	0 (0%)	1 (100%)
No. of patients using propranolol hydrochloride, n (%)	69 (77%)	17 (25%)	23 (33%)	29 (42%)

Values are the median (range) or the number of patients (%).

Propranolol hydrochloride was administered to reduce the heart rate before imaging.

Quantitative evaluation

Edge rise distance

We analyzed 1080 ERDs (3 directions × 4 datasets × 90 patients). The ERD measurement results are presented in Table 2. In patients with a low heart rate, the ERD obtained with standard and SSF2 reconstruction was not significantly different (R-R 40% and R-R 75%: $p > 0.05$). However, in patients with an intermediate heart rate, the ERD at R-R 40% was significantly shorter on SSF2 (2.0 mm)- than standard (2.4 mm) images ($p < 0.001$). In patients whose heart rate was high, the ERD at R-R 40% and R-R 75% was significantly shorter on SSF2- than standard images ($p < 0.001$).

Table 2. Comparison of the edge rise distance (mm) on scans subjected to standard- and SSF2 reconstruction.

	R-R interval	Standard	SSF2	*P*
Patients with low HR (<60 bpm)	40%	1.8 (1.0-4.2)	1.6 (0.9-4.0)	0.067
	75%	1.9 (1.0-4.2)	1.8 (0.9-4.1)	0.122
Patients with intermediate HR (60-69 bpm)	40%	2.4 (0.9-5.1)	2.0 (0.9-4.5)	<0.001
	75%	2.1 (1.0-5.1)	2.1 (0.9-4.1)	0.077
Patients with high HR (>70 bpm)	40%	2.5 (1.1-5.7)	2.0 (1.0-5.2)	<0.001
	75%	2.5 (1.1-5.9)	2.0 (1.0-4.9)	<0.001

HR = heart rate. Values are the median (range).

Dispersion of sizing

As shown in Table 3, the SD of the aortic annulus area was significantly smaller in SSF2 reconstruction than in standard at low (94.7 vs 63.3 and 105.2 vs 78.9)-, intermediate (71.8 vs 47.9 and 90.4 vs 58.3)-, and high heart rate (58.7 vs 45.1 and 70.3 vs 45.8) R-R interval of 40% and 75% (all: $p < 0.05$).

Table 3. Comparison of SD of the aortic annulus areas (mm^2) of scans subjected to standard- and SSF2 reconstruction.

	R-R interval	Standard	SSF2	*P*
Patients with low HR (<60 bpm)	40%	448.7 (94.7)	436.5 (63.3)	0.002
	75%	428.9 (105.2)	435.0 (78.9)	0.029
Patients with intermediate HR (60-69 bpm)	40%	442.1 (71.8)	435.5 (47.9)	0.002
	75%	445.8 (90.4)	439.4 (58.3)	0.001
Patients with high HR (>70 bpm)	40%	437.4 (58.7)	435.8 (45.1)	0.002
	75%	432.3 (70.3)	414.6 (45.8)	0.001

HR = heart rate, bpm = beats per minute. Values are the mean (SD).

As shown in Table 4, the SD of the aortic annulus perimeter was also significantly smaller in SSF2 reconstruction than in standard at low (11.6 vs 7.4 and 9.5 vs 6.0)-, intermediate (9.4 vs 5.6 and 10.8 vs 6.8)-, and high heart rate (8.4 vs 4.3 and 9.3 vs 5.4) R-R interval of 40% and 75% (all: $p < 0.001$).

Table 4. Comparison of SD of the aortic annulus perimeter (mm) of scans subjected to standard- and SSF2 reconstruction.

	R-R interval	Standard	SSF2	*P*
Patients with low HR (<60 bpm)	40%	75.0 (11.6)	75.6 (7.4)	<0.001
	75%	75.4 (9.5)	74.7 (6.0)	<0.001
Patients with intermediate HR (60-69 bpm)	40%	74.6 (9.4)	74.0 (5.6)	<0.001
	75%	77.0 (10.8)	75.7 (6.8)	<0.001
Patients with high HR (>70 bpm)	40%	74.8 (8.4)	73.3 (4.3)	<0.001
	75%	71.5 (9.3)	71.3 (5.4)	<0.001

HR = heart rate, bpm = beats per minute. Values are the mean (SD).

Contrast-to-noise ratio

As shown in Table 5, the CT number of the ascending aorta and the septal wall of the ventricle and the image noise of the ascending aorta showed no significant difference between the two reconstructions, irrespective of the patients' heart rate (all: $p > 0.05$). In addition, these CNR also showed no significant difference between the two reconstructions at low (18.5 vs 19.5, $p = 0.404$)-, intermediate (16.5 vs 16.3, $p = 0.860$)-, and high heart rate (17.6 vs 18.1, $p = 0.312$). The 95% confidence interval for the difference between standard and SSF2 reconstruction was −3.0 to 1.2 in patients with a low heart rate, −2.5 to 2.1 in patients with an intermediate heart rate, and −2.7 to 0.9 in patients with a high heart rate. Because the 95% confidence interval did not cross the bilateral predefined equivalence margin (Fig 2) in all heart rate classes, we

considered CNR to be equivalent among our standard and SSF2 reconstitution irrespective of their heart rate.

Table 5. CT number, image noise and contrast-to-noise ratio at each site.

		Standard	SSF2	*P*
Patients with low HR (<60 bpm)	CT number of the ascending aorta (HU)	401.7 (204.7-478.9)	400.7 (205.0-478.9)	0.928
	Image noise of the ascending aorta	16.9 (13.1-22.3)	16.3 (11.6-22.2)	0.206
	CT number of septal wall of the ventricle (HU)	83.4 (59.5-116.0)	85.6 (56.7-115.0)	0.601
	Contrast-to-noise ratio	18.5 (8.5-24.1)	19.5 (9.0-26.9)	0.404
Patients with intermediate HR (60-69 bpm)	CT number of the ascending aorta (HU)	375.0 (308.8-490.0)	380.6 (299.0-492.5)	0.962
	Image noise of the ascending aorta	17.3 (13.0-26.5)	17.7 (13.0-27.5)	0.818
	CT number of septal wall of the ventricle (HU)	81.1 (55.9-111.1)	82.5 (49.3-115.0)	0.904
	Contrast-to-noise ratio	16.5 (11.5-30.8)	16.3 (9.9-31.0)	0.860
Patients with high HR (>70 bpm)	CT number of the ascending aorta (HU)	400.0 (314.5-531.7)	400.0 (295.5-528.7)	0.885
	Image noise of the ascending aorta	18.1 (15.5-23.5)	17.0 (13.9-22.0)	0.161
	CT number of septal wall of the ventricle (HU)	80.5 (59.5-117.4)	83.4 (56.7-123.2)	0.982
	Contrast-to-noise ratio	17.6 (11.7-24.0)	18.1 (13.3-24.0)	0.312

HR = heart rate, HU = Hounsfield units. Values are the median (range).

Fig 2. Results of the equivalence test. Results of the equivalence test for the difference in CNR between standard and SSF2 reconstruction. CNR = contrast-to-noise ratio; HR = heart rate; SSF2 = SnapShot Freeze 2

Qualitative analysis

Table 6 shows the results of the visual evaluation of MPR images submitted by our two readers. In patients with a low heart rate, at R-R 75%, there was no significant difference in the mean image scores assigned to images subjected to standard- or SSF2 reconstruction ($p = 0.540$). At R-R 40% the visualization scores were significantly higher for images reconstructed with SSF2 than standard (all: $p < 0.01$). There was substantial interobserver agreement with respect to the overall image quality ($\kappa = 0.69$). SSF2 reconstruction improved the image quality of the aortic annulus in the representative case shown in Fig 3.

Table 6. Comparison of the image quality scores of scans subjected to standard- and SSF2 reconstruction.

	R-R interval	Standard	SSF2	*P*
Patients with low HR (<60 bpm)	40%	2.6 (1.1)	3.6 (0.7)	<0.001
	75%	3.9 (0.9)	4.0 (0.7)	0.540
Patients with intermediate HR (60-69 bpm)	40%	2.1 (0.9)	3.5 (0.6)	<0.001
	75%	2.9 (0.8)	3.6 (0.7)	0.003
Patients with high HR (>70 bpm)	40%	2.5 (0.7)	3.7 (0.4)	<0.001
	75%	2.2 (0.7)	3.2 (0.6)	<0.001

HR = heart rate, bpm = beats per minute. Values are the mean (SD).

Fig 3. Clinical image of SSF2. In their 80s (height = 157 cm, body weight = 58 kg, body mass index = 23.5 kg/m^2, heart rate during the scan = 116 bpm (atrial fibrillation). (A) and (C): MPR images of the aortic annulus (R-R interval = 40% and 75%) using standard reconstruction. The visualization scores for A and C were 1 and 2, respectively.

(B) and (D): After SSF2 reconstruction, both visualization scores were 4. The evaluable image quality improved. WW = window width; WL = window level

Discussion

Our study demonstrates that the second-generation whole-heart motion correction algorithm (SSF2) was superior to standard reconstruction with respect to the image quality of pre-TAVI cardiac CT scans acquired for the evaluation of the aortic annulus.

At R-R 40%, SSF2 reconstructed images received significantly higher image quality scores than did standard reconstruction regardless of the patients' heart rate ($p < 0.001$). At R-R 75%, in patients with an intermediate and high heart rate was the visualization score higher for SSF2- than standard reconstructed images. At R-R 40% and R-R 75%, SSF2 strongly tended to yield higher image quality scores than did standard reconstruction. Consequently, SSF2 reconstruction raised the image quality significantly, especially in patients with a high heart rate or a 40% R-R interval.

The earlier vendor-specific motion correction algorithm (SSF1) was designed to address coronary motion artifacts on cardiac scans. It was primarily indicated for coronary imaging and was shown to improve the image quality and diagnostic accuracy of scans performed for the detection of significant coronary stenosis, especially in patients with a high heart rate [12-19]. The SSF2 algorithm extends motion correction to include the whole heart. It is expected to be useful for imaging of not only the coronary arteries but also of other non-coronary intracardiac structures such as the cardiac valves.

Earlier studies that applied SSF2 reconstruction to images of the coronary arteries, of heart- and valve structures, and of the great vessels showed that the image quality was significantly improved by the algorithm and the number of non-evaluable scans was lower than of images subjected to standard- or SSF1 reconstruction [20, 21].

Our study focused on the aortic annulus; it indicates that SSF2 yielded higher motion artifact correction in the whole heart.

Others [29] who applied SSF1 to cardiac CT for aortic annulus measurements reported that it significantly improved the image quality of systolic CT datasets. We examined the effect of SSF2 in a wide range of heart rates and showed that it is useful for the evaluation of the aortic annulus not only in the systolic- but also in the diastolic phase. Our findings suggest that SSF2 reconstruction reduces aortic valve motion artifacts throughout the cardiac phases.

SSF2 reconstruction was not useful at R-R interval 75% in patients with a low or intermediate heart rate. At those heart rates and cardiac phases, the temporal resolution on electrocardiogram-gated scans may be sufficient and motion artifacts may not be inherent. SSF1- and SSF2 reconstruction may be useful in patients with a high heart rate and for scans with low temporal resolution [12, 13, 20, 21]. Our findings suggest that SSF2 is as useful as SSF1 in patients with a high heart rate.

Although cardiac CT is the reference standard for the workup of TAVI candidates scheduled for an investigation of the aortic root [1, 2], motion artifacts reduce the accuracy of aortic annulus sizing and directly impact on patient outcome after TAVI procedure [2, 7-9]. As a result of evaluating the dispersion between the two reconstructions with respect to the sizing of the aortic annulus, SSF2 was significantly smaller than standard regardless of the patients' heart rate or R-R interval. For TAVI planning, we still tend to use systolic imaging for the measurements [2, 4, 29, 30] and the aortic annulus seems to be better delineated when SSF2 is used. Therefore, SSF2 may contribute to improving the accuracy of sizing of the aortic annulus.

As renal dysfunction is relatively common in elderly patients scheduled for

TAVI, a low-contrast protocol is recommended [36]. SSF2 reconstruction may be appropriate in TAVI candidates with renal dysfunction because it not only improves the image quality but also reduces the need for rescanning.

To avoid the potential impact of SSF2 reconstruction on quantitative measurements of the ERD, we measured the CT number in the ascending aorta, the image noise, and the CNR on SSF2 reconstructed images. We found that CNR was equivalent between scans subjected to standard- or SSF2 reconstruction irrespective of the patients' heart rate, confirming that SSF2 corrected only the motion artifacts and that it did not affect other parameters.

Our study has some limitations. We only focused on the aortic annulus and did not investigate the effect of SSF2 on other cardiac structures such as the coronary arteries. Areas of calcification were excluded from our quantitative evaluation because their CT attenuation fluctuates significantly. Severe aortic valve calcification could reduce the sizing accuracy of the aortic annulus and further study is required to evaluate whether SSF2- is superior to standard reconstruction in patients with severe aortic valve calcification. Lastly, we did not investigate the relationship between SSF2 and the radiation dose. Additional studies are underway to determine whether the robustness of SSF2 reconstruction allows lowering the preset padding range prior to scanning, thereby minimizing the required radiation dose.

Conclusions

In conclusion, our findings suggest that the SSF2 algorithm was superior to standard reconstruction because it improved the image quality and reduces motion artifacts especially in patients with a high heart rate or a 40% R-R interval. These findings may help SSF2 improve the accuracy of sizing of the aortic annulus prior to TAVI.

Supporting information

S1 Table. Raw data for each group. (XLSX)

References

1. Schuhbaeck A, Achenbach S, Pflederer T, Marwan M, Schmid J, Nef H, et al. Reproducibility of aortic annulus measurements by computed tomography. Eur Radiol. 2014;24(8):1878-88.

2. Achenbach S, Delgado V, Hausleiter J, Schoenhagen P, Min JK, Leipsic JA. SCCT expert consensus document on computed tomography imaging before transcatheter aortic valve implantation (TAVI)/transcatheter aortic valve replacement (TAVR). J Cardiovasc Comput Tomogr. 2012;6(6):366-80.

3. Andreini D, Pontone G, Mushtaq S, Mancini ME, Conte E, Guglielmo M, et al. Image quality and radiation dose of coronary CT angiography performed with whole-heart coverage CT scanner with intra-cycle motion correction algorithm in patients with atrial fibrillation. Eur Radiol. 2018;28(4):1383-92.

4. Binder RK, Webb JG, Willson AB, Urena M, Hansson NC, Norgaard BL, et al. The impact of integration of a multidetector computed tomography annulus area sizing algorithm on outcomes of transcatheter aortic valve replacement: a prospective, multicenter, controlled trial. J Am Coll Cardiol. 2013;62(5):431-8.

5. Harris BS, De Cecco CN, Schoepf UJ, Steinberg DH, Bayer RR, Krazinski AW, et al. Dual-source CT imaging to plan transcatheter aortic valve replacement: accuracy for diagnosis of obstructive coronary artery disease. Radiology. 2015;275(1):80-8.

6. Kodali S, Thourani VH, White J, Malaisrie SC, Lim S, Greason KL, et al. Early clinical and echocardiographic outcomes after SAPIEN 3 transcatheter aortic valve replacement in inoperable, high-risk and intermediate-risk patients with aortic stenosis. Eur Heart J. 2016;37(28):2252-62.

389 7. Makkar RR, Fontana GP, Jilaihawi H, Kapadia S, Pichard AD, Douglas PS, et
390 al. Transcatheter aortic-valve replacement for inoperable severe aortic stenosis. N Engl J
391 Med. 2012;366(18):1696-704.
392 8. Holmes DR, Jr., Mack MJ, Kaul S, Agnihotri A, Alexander KP, Bailey SR, et al.
393 2012 ACCF/AATS/SCAI/STS expert consensus document on transcatheter aortic valve
394 replacement. J Am Coll Cardiol. 2012;59(13):1200-54.
395 9. Schmidkonz C, Marwan M, Klinghammer L, Mitschke M, Schuhbaeck A,
396 Arnold M, et al. Interobserver variability of CT angiography for evaluation of aortic
397 annulus dimensions prior to transcatheter aortic valve implantation (TAVI). Eur J Radiol.
398 2014;83(9):1672-8.
399 10. Leipsic J, Abbara S, Achenbach S, Cury R, Earls JP, Mancini GJ, et al. SCCT
400 guidelines for the interpretation and reporting of coronary CT angiography: a report of
401 the Society of Cardiovascular Computed Tomography Guidelines Committee. J
402 Cardiovasc Comput Tomogr. 2014;8(5):342-58.
403 11. Aghayev A, Murphy DJ, Keraliya AR, Steigner ML. Recent developments in
404 the use of computed tomography scanners in coronary artery imaging. Expert Rev Med
405 Devices. 2016;13(6):545-53.
406 12. Liang J, Wang H, Xu L, Dong L, Fan Z, Wang R, et al. Impact of SSF on
407 Diagnostic Performance of Coronary Computed Tomography Angiography Within 1
408 Heart Beat in Patients With High Heart Rate Using a 256-Row Detector Computed
409 Tomography. J Comput Assist Tomogr. 2018;42(1):54-61.
410 13. Wen B, Xu L, Liang J, Fan Z, Sun Z. A Preliminary Study of Computed
411 Tomography Coronary Angiography Within a Single Cardiac Cycle in Patients With
412 Atrial Fibrillation Using 256-Row Detector Computed Tomography. J Comput Assist

413 Tomogr. 2018;42(2):277-81.

414 14. Liang J, Wang H, Xu L, Yang L, Dong L, Fan Z, et al. Diagnostic performance
415 of 256-row detector coronary CT angiography in patients with high heart rates within a
416 single cardiac cycle: a preliminary study. Clin Radiol. 2017;72(8):694 e7- e14.

417 15. Sheta HM, Egstrup K, Husic M, Heinsen LJ, Nieman K, Lambrechtsen J.
418 Impact of a motion correction algorithm on image quality in patients undergoing CT
419 angiography: A randomized controlled trial. Clin Imaging. 2017;42:1-6.

420 16. Sheta HM, Egstrup K, Husic M, Heinsen LJ, Lambrechtsen J. Impact of a
421 motion correction algorithm on quality and diagnostic utility in unselected patients
422 undergoing coronary CT angiography. Clin Imaging. 2016;40(2):217-21.

423 17. Machida H, Lin XZ, Fukui R, Shen Y, Suzuki S, Tanaka I, et al. Influence of
424 the motion correction algorithm on the quality and interpretability of images of
425 single-source 64-detector coronary CT angiography among patients grouped by heart
426 rate. Jpn J Radiol. 2015;33(2):84-93.

427 18. Lee H, Kim JA, Lee JS, Suh J, Paik SH, Park JS. Impact of a vendor-specific
428 motion-correction algorithm on image quality, interpretability, and diagnostic
429 performance of daily routine coronary CT angiography: influence of heart rate on the
430 effect of motion-correction. Int J Cardiovasc Imaging. 2014;30(8):1603-12.

431 19. Leipsic J, Labounty TM, Hague CJ, Mancini GB, O'Brien JM, Wood DA, et al.
432 Effect of a novel vendor-specific motion-correction algorithm on image quality and
433 diagnostic accuracy in persons undergoing coronary CT angiography without
434 rate-control medications. J Cardiovasc Comput Tomogr. 2012;6(3):164-71.

435 20. Liang J, Sun Y, Ye Z, Sun Y, Xu L, Zhou Z, et al. Second-generation motion
436 correction algorithm improves diagnostic accuracy of single-beat coronary CT

437 angiography in patients with increased heart rate. Eur Radiol. 2019;29(8):4215-27.

438 21. Sun J, Okerlund D, Cao Y, Li H, Zhu Y, Li J, et al. Further Improving Image
439 Quality of Cardiovascular Computed Tomography Angiography for Children With High
440 Heart Rates Using Second-Generation Motion Correction Algorithm. J Comput Assist
441 Tomogr. 2020;44(5):790-5.

442 22. Mushtaq S, Conte E, Melotti E, Andreini D. Coronary CT Angiography in
443 Challenging Patients: High Heart Rate and Atrial Fibrillation. A Review. Acad Radiol.
444 2019;26(11):1544-9.

445 23. Le Roy J, Zarqane H, Azais B, Vernhet Kovacsik H, Mura T, Okerlund D, et al.
446 Impact of Motion Correction Algorithms on Image Quality in Children Undergoing
447 Coronary Computed Tomography Angiography: A Comparison With Regular
448 Monophasic and Multiphasic Acquisitions. Circ Cardiovasc Imaging.
449 2019;12(12):e009650.

450 24. Fuchs TA, Stehli J, Dougoud S, Fiechter M, Sah BR, Buechel RR, et al. Impact
451 of a new motion-correction algorithm on image quality of low-dose coronary CT
452 angiography in patients with insufficient heart rate control. Acad Radiol.
453 2014;21(3):312-7.

454 25. Lell MM, Kachelriess M. Recent and Upcoming Technological Developments
455 in Computed Tomography: High Speed, Low Dose, Deep Learning, Multienergy. Invest
456 Radiol. 2020;55(1):8-19.

457 26. Greffier J, Hamard A, Pereira F, Barrau C, Pasquier H, Beregi JP, et al. Image
458 quality and dose reduction opportunity of deep learning image reconstruction algorithm
459 for CT: a phantom study. Eur Radiol. 2020;30(7):3951-9.

460 27. Solomon J, Lyu P, Marin D, Samei E. Noise and spatial resolution properties of

461 a commercially available deep learning-based CT reconstruction algorithm. Med Phys.
462 2020;47(9):3961-71.
463 28. Benz DC, Benetos G, Rampidis G, von Felten E, Bakula A, Sustar A, et al.
464 Validation of deep-learning image reconstruction for coronary computed tomography
465 angiography: Impact on noise, image quality and diagnostic accuracy. J Cardiovasc
466 Comput Tomogr. 2020;14(5):444-51.
467 29. Soon J, Sulaiman N, Park JK, Kueh SH, Naoum C, Murphy D, et al. The effect
468 of a whole heart motion-correction algorithm on CT image quality and measurement
469 reproducibility in Pre-TAVR aortic annulus evaluation. J Cardiovasc Comput Tomogr.
470 2016;10(5):386-90.
471 30. Apfaltrer P, Henzler T, Blanke P, Krazinski AW, Silverman JR, Schoepf UJ.
472 Computed tomography for planning transcatheter aortic valve replacement. J Thorac
473 Imaging. 2013;28(4):231-9.
474 31. Rixe J, Schuhbaeck A, Liebetrau C, Moellmann H, Nef HM, Szardien S, et al.
475 Multi-detector computed tomography is equivalent to trans-oesophageal
476 echocardiography for the assessment of the aortic annulus before transcatheter aortic
477 valve implantation. Eur Radiol. 2012;22(12):2662-9.
478 32. Tatsugami F, Higaki T, Sakane H, Fukumoto W, Kaichi Y, Iida M, et al.
479 Coronary Artery Stent Evaluation with Model-based Iterative Reconstruction at
480 Coronary CT Angiography. Acad Radiol. 2017;24(8):975-81.
481 33. Tatsugami F, Higaki T, Nakamura Y, Yu Z, Zhou J, Lu Y, et al. Deep
482 learning-based image restoration algorithm for coronary CT angiography. Eur Radiol.
483 2019;29(10):5322-9.
484 34. Gupta AK, Nelson RC, Johnson GA, Paulson EK, Delong DM, Yoshizumi TT.

485 Optimization of eight-element multi-detector row helical CT technology for evaluation
486 of the abdomen. Radiology. 2003;227(3):739-45.
487 35. Piaggio G, Elbourne DR, Pocock SJ, Evans SJ, Altman DG, Group C.
488 Reporting of noninferiority and equivalence randomized trials: extension of the
489 CONSORT 2010 statement. JAMA. 2012;308(24):2594-604.
490 36. Geyer LL, De Cecco CN, Schoepf UJ, Silverman JR, Krazinski AW, Bamberg
491 F, et al. Low-volume contrast medium protocol for comprehensive cardiac and
492 aortoiliac CT assessment in the context of transcatheter aortic valve replacement. Acad
493 Radiol. 2015;22(9):1138-46.
494

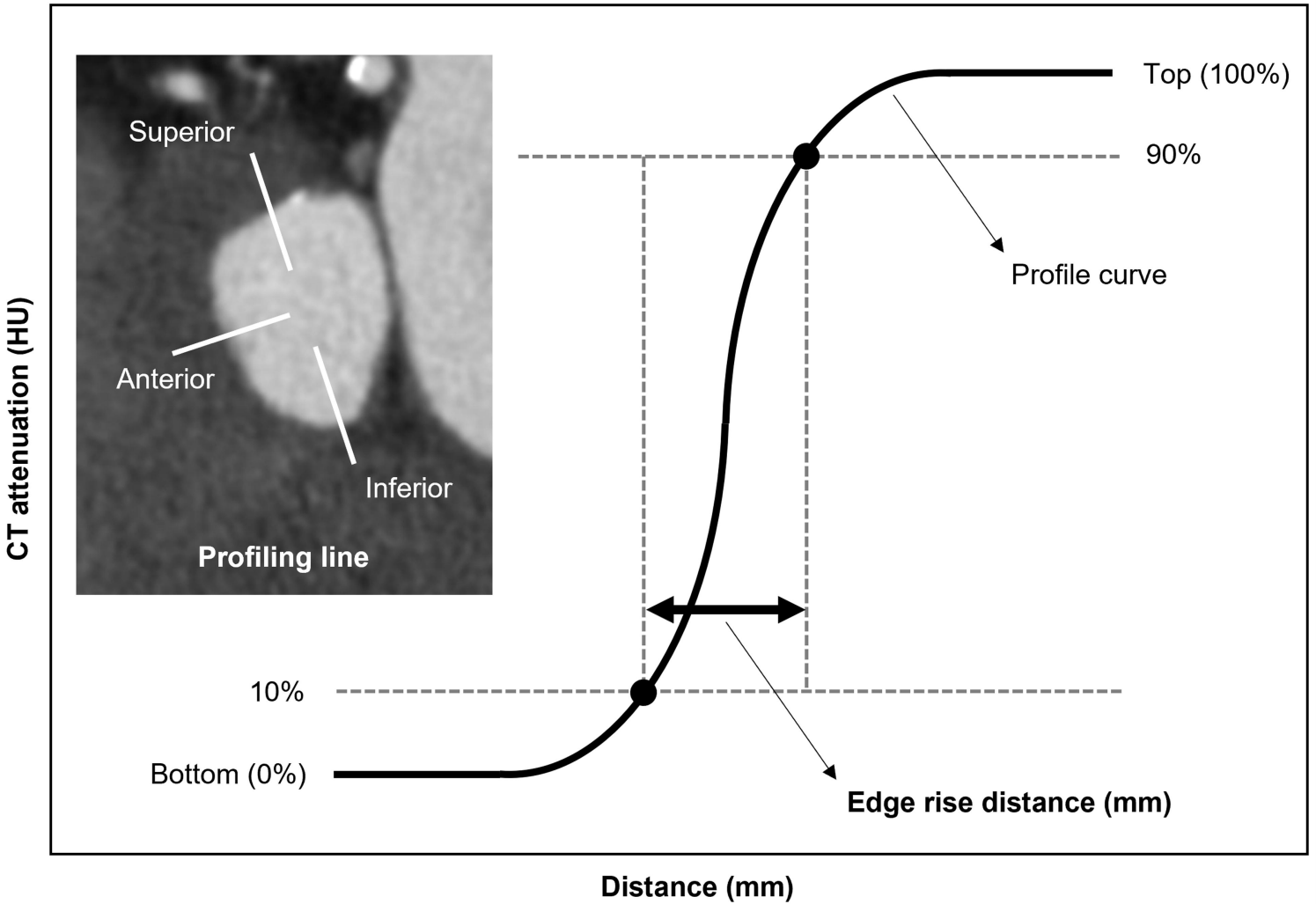
Superior
Anterior
Inferior
Profiling line
Top (100%)
90%
Profile curve
10%
Bottom (0%)
Edge rise distance (mm)
CT attenuation (HU)
Distance (mm)

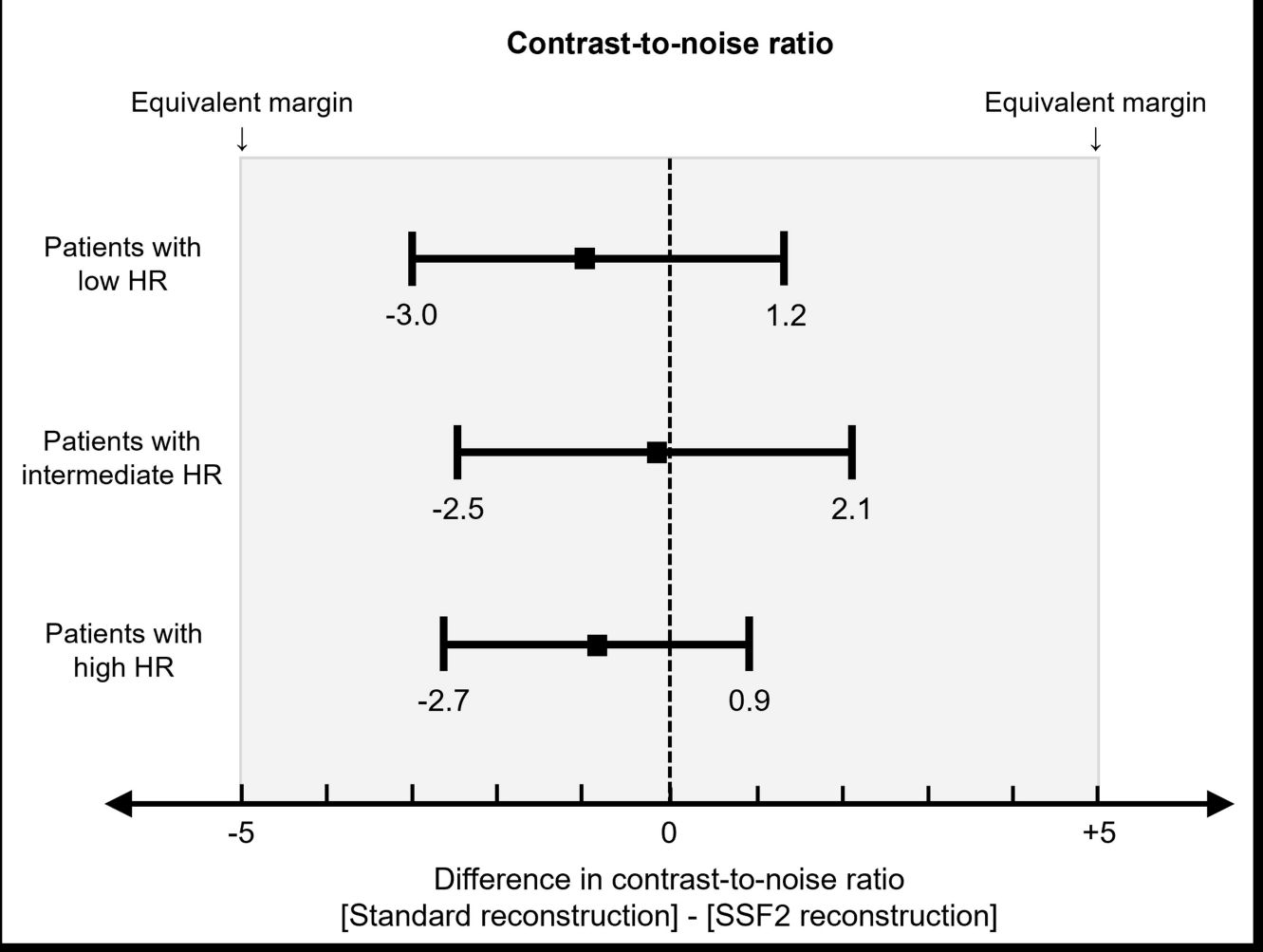
Contrast-to-noise ratio
Equivalent margin
Equivalent margin
Patients with low HR
-3.0
1.2
Patients with intermediate HR
-2.5
2.1
Patients with high HR
-2.7
0.9
-5
0
+5
Difference in contrast-to-noise ratio
[Standard reconstruction] - [SSF2 reconstruction]

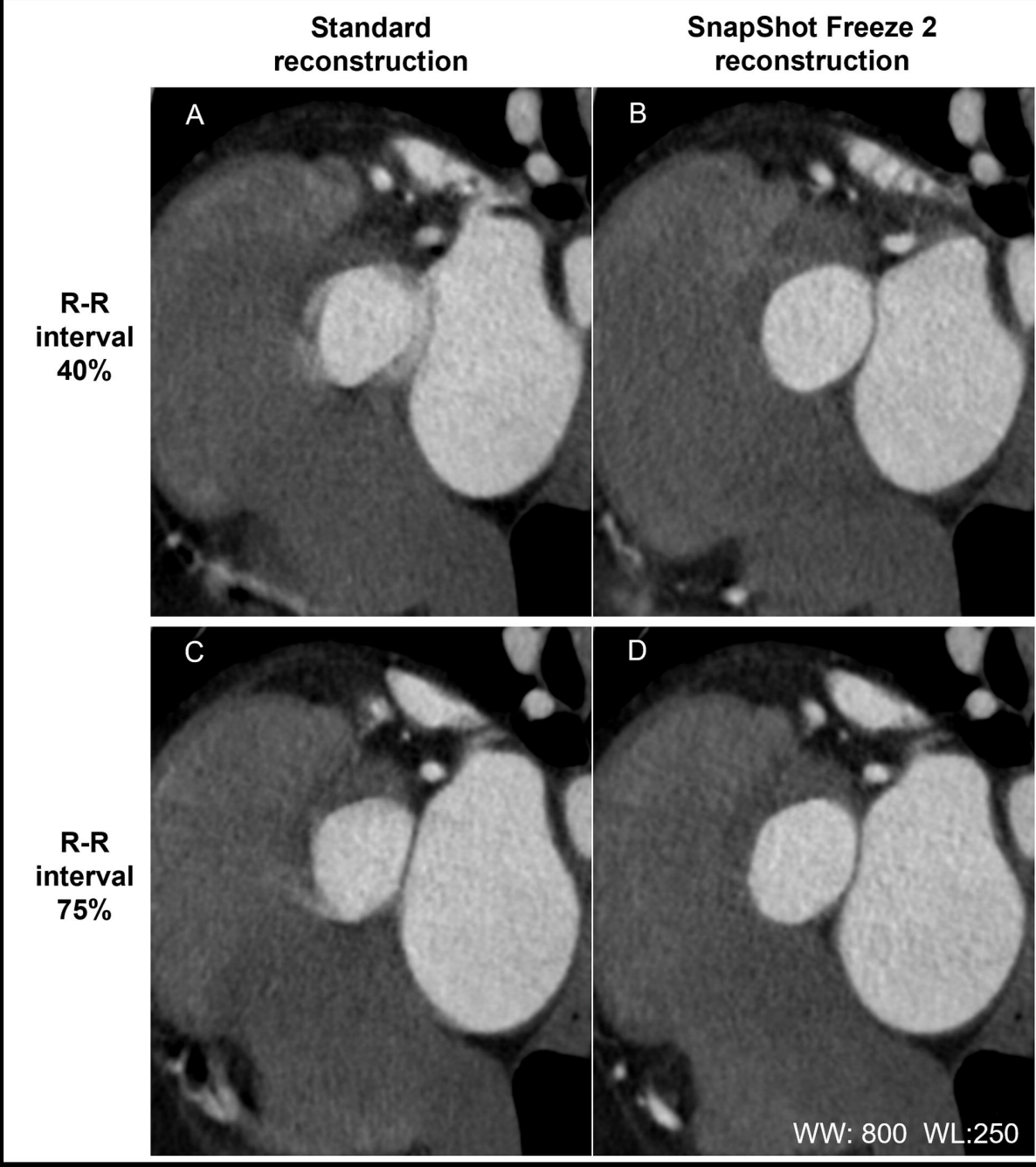
Standard reconstruction
SnapShot Freeze 2 reconstruction
R-R interval 40%
R-R interval 75%
A
B
C
D
WW: 800 WL:250